Polycaprolactone/organoclay biodegradable nanocomposites: Dissimilar tendencies of different clay modifiers

Romina P. Ollier, Matias R. Lanfranconi, Vera A. Alvarez, Leandro N. Ludueña*

Materiales Compuestos Termoplásticos (CoMP), Instituto de Investigaciones en Ciencia y Tecnología de Materiales (INTEMA), CONICET - Universidad Nacional de Mar del Plata (UNMdP). Av. Colón 10890, Mar del Plata, 7600, Argentina.

*Corresponding author

DOI: 10.5185/amlett.2018.1828
www.vbripress.com/aml

Abstract

In this work, biodegradable nanocomposites based on polycaprolactone (PCL) reinforced with 2.5, 5.0 and 7.5 wt.% of two different clays, a commercial organo-clay (Cloisite 20A, C20A) and a laboratory modified bentonite with tributylhexadecyl phosphonium bromide (bTBHP), were prepared by melt intercalation followed by compression molding. The study contemplates the analysis of chemical (Infrared Spectrometry, FTIR), morphological (X-Ray Diffractometry, XRD, Scanning Electron Microscopy, SEM, and Transmission Electron Microscopy, TEM), rheological, thermal (Differential Scanning Calorimetry, DSC, and Thermogravimetrical Analysis, TGA) and mechanical properties (tensile tests), which are important properties for packaging applications.

In previous works, we concluded that higher clay dispersion degree inside the PCL matrix is expected when clays with large interlayer distance, strong hydrophobicity and strong processing stability are used. In the present work the opposite result was obtained. Although the phosphonium treated clay (bTBHP) showed the largest interlayer distance (d_{001}), strongest hydrophobicity and the best processing stability, the clay dispersion degree inside PCL was worse than in the case of the alkylammonium treated clay (C20A). PCL/bTBHP nanocomposites showed weaker mechanical properties in comparison with PCL/C20A ones, which is in accordance with the morphological analysis. On the other hand, the thermal properties of the matrix were not substantially affected by clay incorporation in both nanocomposites.

Keywords: Nanocomposites, compatibility, biodegradable polymer, bentonite, montmorrillonite.

Introduction

The development of environmental friendly, biodegradable, polymeric materials has attracted extensive interest in the last decades due to the pollution caused by the waste accumulation at the end of the life cycle of traditional polymer products **[1-4]**. Polycaprolactone (PCL) is a chemically synthesized aliphatic polyester which does not occur in nature but it is fully biodegradable **[5-6]**. It has low glass transition (-60 ºC) and melting (60 ºC) temperatures **[7]**. It can be processed by conventional techniques such as extrusion, injection molding, blow molding, thermoforming and calendering. Although PCL has been broadly used as matrix for the design of biodegradable nanocomposites for medical and packaging applications, in certain cases it is not competitive enough compared with conventional thermoplastics because some of its properties are limited **[8]**. The performance of this polymer can be greatly enhanced by the addition of a small amount (typically less than 10 wt.%) of nanometer-size inorganic fillers, such as layered silicates, producing nanocomposites **[1, 3, 5, 9-16]**.

A key factor in the preparation of nanocomposites is to compatibilize the matrix and the filler, which will affect the nanostructure of the resulting material. In order to achieve the best properties it is necessary to obtain a totally exfoliated structure, in which the individual clay platelets are completely and uniformly dispersed in the polymeric matrix. However, instead of fully exfoliated structures, intercalated structures (where the polymer chains are inserted between the platelets, increasing the interlayer distance, but without separating them completely) or a mixture of both, are generally achieved **[17]**. Hence, the characterization of the clay morphology (dispersion and distribution) inside the polymer matrix is crucial to understand these materials.

Smectite clays have increasingly attracted research interests for the preparation of polymer/clay nanocomposites in the past decade. Two important clays, due to environmental and economic relevance and mechanical and chemical resistance, are bentonite (bent) and montmorillonite (MMT). These smectite clays of about 1 nm in thickness are the clays of choice for polymer nanocomposite production **[18]**. As it was

previously mentioned, the efficiency of the clays to enhance the properties of the polymer matrix, depends on the degree of the dispersion of the platelets. Because most polymers are organophilic, the hydrophilic nature of clays hinders the exfoliation of the silicate layers. However, due to the rich intercalation and ion-exchange chemistry of bent and MMT, they can be organically modified in order to achieve a better compatibility with the matrix. The interlayer ions can be easily exchanged by organic ions, mainly ammonium or phosphonium cations having aliphatic or aromatic short or long alkyl chains, in order to produce an increment in the interlayer spacing (d_{001}) and reduce the hydrophilicity of the clay **[19-22]**. The resulting organo-modified clays have less surface energy and they are more compatible with hydrophobic polymers, which promotes interactions that facilitate the insertion of the polymer chains inside the clay galleries under defined processing conditions **[19, 23]**.

A number of research articles have been reported in the literature concerning the preparation and properties of PCL/clay nanocomposites using different commercially available organo-modified clay minerals. Chen *et al.* **[2]** have prepared intercalated PCL/clay nanocomposites with organo-modified montmorillonite up to 30 wt.%. They also prepared microcomposites with 58.5 wt % of natural montmorillonite and suggests that it is not the largest clay loading that PCL with a molecular weight of 80,000 can sustain. Janigová et al. **[24]** have prepared PCL/clay nanocomposites by melt blending. Natural montmorillonite (MMT) and two montmorillonite clays modified with dimethyl, benzyl, hydrogenated tallow, quaternary ammonium (2MBHT) and dimethyl, dehydrogenated tallow, quaternary ammonium (2M2HT) were used as fillers. It must be mentioned that the supplier of these clays (Southern clay products) recommends an initial screening for the selection of their Cloisite® products relative to the hydrophobicity/hydrophilicity hydrophobic/hydrophilic nature of the system. The authors of this work demonstrated by TEM and XRD lower dispersion degree for PCL/Cloisite® 15A nanocomposites and almost the same Young's modulus than PCL/Cloisite 10A® nanocomposites. They did not analyze the effect of the PCL/clay hydrophobicity/hydrophilicity nature and the initial clay interlayer distance on these results but it can be observed on the web page of the supplier that Cloisite® 15A is more hydrophobic and has higher interlayer distance than Cloisite 10A®, so, the results were opposite as those expected. Zheng et al. **[2, 25]** and Lepoittevin et al. **[1]** obtained similar results. They have prepared PCL based nanocomposites by melt blending using Cloisite® 30B and Cloisite® 15A **[25]**; and Cloisite® 30B and Cloisite® 25A **[1]**, respectively, as fillers. In both works they obtained the highest clay dispersion degree with PCL/Cloisite® 30B nanocomposites and they did not find substantial differences in the mechanical properties between the different nanocomposites even when Cloisite® 15A and Cloisite® 25A are more hydrophobic and have larger interlayer distance than Cloisite® 30B. Chen et al. **[2]** prepared PCL/clay nanocomposites by melt processing. They used natural sodium montmorillonite from Blackhill Bentonite LLC and two montmorillonite clays modified with benzyl-2-methyl-hydrogenated tallow quaternary ammonium chloride (NH_4MMT2) and 2-methyl-2-hydrogenated tallow quaternary ammonium chloride (NH_4MMT1) from Elementis Specialties, which are the same modifiers as those used in Cloisite® 10A and Cloisite® 20A, respectively. It was proved by XRD that the interlayer distance of NH_4MMT2 was lower than that of NH_4MMT1. On the other hand, the hydrophobicity/hydrophilicity nature of the system was not analyzed but the available information about Cloisite® 10A and Cloisite® 20A suggests that NH_4MMT1 is more suitable as filler of PCL than NH_4MMT2. Even so, the nanocomposites prepared with NH_4MMT2 showed the highest clay dispersion degree and led to the greater enhancement of the Young´ s modulus of the PCL at low filler loading. Recently, Yahiaoui et al. **[8]** elaborated antimicrobial PCL-based nanocomposite films by melt mixing process using two quaternary ammonium-modified montmorillonites.

In previous works, we tried to explain these tendencies analyzing the effect of several commercial organo-modified MMT **[9, 26-27]** and a laboratory organo-modified bentonite **[28]** on the morphology and mechanical properties of PCL/clay nanocomposites prepared by melt intercalation and casting. PCL/commercial organo-MMT nanocomposites films were successfully prepared by melt intercalation in a double screw extruder followed by compression molding. The results suggested that the main characteristics responsible for the final morphology and properties of the PCL/clay nanocomposites are the hydrophobic/hydrophilic nature of the system, the initial basal spacing of the clay and the processing stability of the clay organo-modifiers.

The aim of this work was to characterize and compare morphological, thermal and mechanical properties of PCL/clay nanocomposites prepared by melt mixing. Two organically-modified clays were used: a commercially organo-MMT, modified with a quaternary ammonium salt (Cloisite 20A), and a bentonite containing a quaternary alkylphosphonium salt as modifier. This work attempts to deeper understand the effect of processing and clay characteristics on the morphology and final properties of polymer/clay nanocomposites in order to contribute with new tools to explain the dissimilar tendencies found in the literature.

Experimental

Materials

PCL provided by Sigma Aldrich (Mn 80,000, Mn/Mw < 2, Glass Transition -60 °C, Melting Temperature 60 °C, Density 1.145 g/mL at 25 °C) was used as matrix. Cloisite® 20A (C20A, Southern Clay Products)

and bentonite (bent, Minarmco S.A.) were used as fillers. The bentonite used in this study consisted predominantly of montmorillonite as evidenced by X-ray diffraction (XRD) analysis **[29]**. It contained quartz and feldspar as major impurities, as well as traces of gypsum and sepiolite. The basal spacing of bent was 1.3 nm and its cation exchange capacity (CEC) was 0.939 meq.g^{-1} **[29]**. The bentonite was organo-modified with tributylhexadecylphosphonium bromide (TBHP) (Sigma Aldrich). All these commercial chemicals were used as received without further purification.

Material synthesis

Modification of bentonite with TBHP **[29]**. Firstly, 2.5 g of bentonite were dispersed in 100 ml of deionised water. Then, an aqueous solution of the corresponding concentration of TBHP (0.9 times the CEC of the bentonite) was added to the suspension. The mixture was stirred for 4 hours at 70 ºC. After that, the suspension was filtered through a Buchner Funnel and washed several times with deionesed water until free of bromide. The wet organoclay, named bTBHP, was frozen for 24 hours and then lyophilized at 100 mTorr and −50 °C for 72 hours using a VirTis 2KBTES-55 freeze dryer.

Preparation of nanocomposites

Neat polymer and nanocomposites with 2.5, 5.0 and 7.5 wt.% of each clay were prepared by melt-intercalation followed by compression-moulding. An intensive Brabender type mixer with two counter-rotating roller rotors was used. Mixing temperature was 100 ºC; speed of rotation was 150 r.p.m. and mixing time was 10 minutes. Compression moulding was carried out to prepare sheets in a hydraulic press for 10 minutes at 100 ºC. The thickness of the sheets was between 0.3-0.5 mm.

The samples will be referred as xbTBHP and xC20A, being x the wt.% content of bTBHP and C20A, respectively, in the nanocomposites.

Characterization of organoclays and nanocomposites

X-Ray diffractometry (XRD) of clay powders and nanocomposites was performed using a PANalytical X'Pert PRO diffractometer equipped with CuKα radiation (λ=1.5406 Å) operating at 40 kV and 40 mA, at a scanning speed of 1 °/min. The basal spacing distances (d_{001}) of the clays were calculated from the 2θ values using the Bragg's equation.

Thermogravimetric Analysis (TGA) measurements were carried out by using a TA Auto-MTGA Q500 Hi-Res. The samples were heated from 30 °C to 900 °C with a heating rate of 10 °C/min under air atmosphere. Tests were performed for neat organoclays, in order to measure the organic content, calculated as the weight change between 200 and 500 ºC. Derivative thermogravimetrical analysis (DTGA) was performed to calculate the temperatures for the maximum thermal degradation rate (*Tp*) of the clay organomodifiers; and to measure the temperature corresponding to 5 wt. % of mass loss ($T_{d5\%}$) and the residual mass at 900 °C for the nanocomposites.

Infrared Spectroscopy (FTIR) spectra of pristine PCL and the nanocomposites were obtained on a Perkin–Elmer Spectrophotometer model Spectrum 100 in attenuated total reflection (ATR) mode. Spectra, averaged over 16 scans, were taken in the range of 4000–600 cm^{-1} with a resolution of 4 cm^{-1}. It is important to note that the spectra of both sides of all the films displayed the same number of peaks at identical positions with the same relative intensities.

Water absorption tests were carried out at 90 % relative humidity (RH) (simulated from a water solution of 34 wt. % of glycerin). Before tests, all the samples were dried under vacuum until constant weight. Samples were weighted at prefixed times and the absorption at each time was calculated as:

$$M_t(\%) = \frac{M_t - M_0}{M_0}.100 \quad (1)$$

were *Mt* is the mass of the sample at a time *t* and M_0 is the initial mass of the sample (dried).

Differential Scanning Calorimetry (DSC) measurements were performed in a TA Instruments model Q2000 calorimeter, operating from 25 to 100 ºC at a heating rate of 10 ºC/min under nitrogen atmosphere (ASTM D3417-83). The degree of crystallinity (*Xcr*) of each sample was calculated from the following equation, with the assumption that the heat of fusion is proportional to the crystalline content:

$$X_{cr}(\%) = \frac{\Delta H_f}{w_{PCL} \times \Delta H_{100}} \times 100 \quad (2)$$

where ΔH_f is the experimental heat of fusion, wPCL is the PCL weight fraction and ΔH_{100} is the heat of fusion of 100 % crystalline PCL and its value is 136.1 J/g **[30]**. The melting temperature (*Tm*) of each sample was also obtained.

Tensile tests were performed with a universal testing machine Instron 3369 at a constant crosshead speed of 50 mm/min. Samples were prepared according to the ASTM D882-91 standard. Tests were carried out at room temperature. At least five specimens were tested for each sample.

Rheological tests were conducted in an Anton Paar rheometer under nitrogen atmosphere. Plate-plate geometry with a plate diameter of 25 mm was used. Samples were inserted and heated up to 80 °C. Low shear amplitude (2 %) was used in order to avoid the destruction of any stabilized clay structure and to work in the lineal viscoelastic regime. Data were taken for shear rates (γ) in the range of 0.002 to10 s^{-1}. The melt rheology curves were fitted to the power law expression for γ in the range of 0.002-0.030 s^{-1}:

$$\eta = A_{Rh} \cdot \dot{\gamma}^{(n_{Rh})} \quad (3)$$

where the *Rh* subscript represents a rheology parameter, η is the complex viscosity; A_{Rh} a preexponential factor; γ the shear rate and n_{Rh} the shear thinning exponent. In the double logarithmic plot a linear zone at low shear rates (γ up to 0.030 s^{-1} for our both test conditions and polymer/clay system) can be seen. The n_{Rh} parameter was calculated from the slope of this region **[31]**.

Scanning electron microscopy (SEM) measurements were conducted on a JEOL JSM-6460 LV equipment. The samples were fractured in liquid nitrogen, and then were sputter-coated with a thin layer of gold palladium alloy prior to SEM observation.

Transmission Electron Microscopy (TEM) was performed at JEOL CX II using an acceleration voltage of 80 kV, to observe the dispersion of clay platelets within the polymer matrix.

Results and discussion

Physicochemical and structural characterization of the organoclays

The organic treatment of the clay is one of the key factors that influences the nanostructure of composite materials, as it is essential for dispersing the normally hydrophilic clay inside a hydrophobic polymer matrix **[32]**. **Table 1** shows the chemical structure of both alkylammonium and alkylphosphonium cations and summarizes the equilibrium water uptake percentage measured in a 90 % RH environment (M_{24h}), the interlaminar spacing (d_{001}) calculated by XRD, the organic content and the temperature for the maximum degradation rate (*Tp*) assessed by performing thermogravimetric analysis of both organo-modified clays used in this work.

Table 1. Characteristics of the organoclays used as reinforcement of PCL.

Clay	Chemical structure of the organic modifier	*Organic Content* (%)	d_{001} (nm)	M_{24h} (%)	*Tp* (º C)
bTBHP	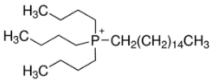	29	2.51	2.73	388
C20A	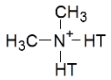	41	2.42	3.72	303

HT: hydrogenated tallow (65% C18; 30% C16; 5% C14)

Regarding XRD characterization, C20A organoclay exhibits almost identical interlaminar spacing compared to the bTBHP organoclay. Hence, in both clays, the polymer chains could have enough space to enter between the clay platelets, which is important in order to obtain a well dispersed nanocomposite **[26]**. On the other hand, the bTBHP organoclay presents lower organic content than C20A, which suggests that the phosphonium salt was more effective improving the clay interlayer distance.

The moisture absorption after 24 hours at an environment with 90 % RH provides information about the bulk polarity of the organoclay, which is important to evaluate the compatibility with the host polymer matrix **[26]**. Taking into account that PCL is a hydrophobic polymer, both organoclays are good candidates for the preparation of PCL nanocomposites because of their low moisture content (in the same conditions pristine montmorillonite and bentonite absorb 12.9 and 19.7 % moisture respectively **[27-28]**).

Another important parameter is the thermal stability of the organoclay **[27]**. The thermal stability of alkylammonium treated organoclays, characterized by the *Tp* values, is in the range of processing temperatures of several traditional polymers. Several studies are focused on the improvement of the thermal stability of organophillic clays which could be useful in the preparation of thermoplastic/clay nanocomposites by melt blending *[33-35]*. Phosphonium salts behave differently than their ammonium counterparts because of the greater steric tolerance of the phosphorus atom and the participation of its low-lying d-orbitals in the processes of making and breaking chemical bonds **[21]**. That is why bTBHP has a remarkable better thermal stability than C20A. In the present work, the processing temperature does not exceed 120 °C, thus, the thermal stability of both organoclays is adequate for the preparation of the PCL nanocomposites. However, it is important to remark that the shear forces developed in the mixing process, together with the high viscosity of the molten polymer, may cause an increase in the melt temperature by viscous dissipation; therefore, the clay modifiers may degrade, both thermal and mechanically, in some extent **[27]**.

Characterization of PCL/organoclay nanocomposites chemical and morphological characterization

The XRD patterns of neat organoclays and PCL/clay nanocomposite samples are shown in **Fig. 1**. As it was previously mentioned, bTBHP and C20A show a 001 diffraction peak corresponding to an interlaminar spacing of 2.51 and 2.42 nm, respectively. All the prepared PCL nanocomposites containing clays with different chemical treatments, exhibited an increase of the d-value of the clay compared to the pure organoclays, which is an indication of intercalation of the polymer chains between the clay platelets **[15]**. This in turns indicates that regardless the organoclay concentration, PCL chains have intercalated into the layers of the bTBHP and C20A modified silicates **[8]**. The highest d_{001} value was observed at the highest clay content of each nanocomposite type. This result suggests that both clays do not agglomerate at 7.5 wt.% inside the PCL matrix in the processing conditions used in this work. The extent of intercalation cannot be quantified by this technique but it must be noted that the d_{001} values of C20A are 7%, 2% and 3% higher than bTBHP ones at 2.5 wt.%, 5.0 wt%, and 7.5 wt.% of clay content, respectively, suggesting highest clay dispersion degree for the C20A nanocomposites. Other

characterization techniques were also used to analyze clay morphology.

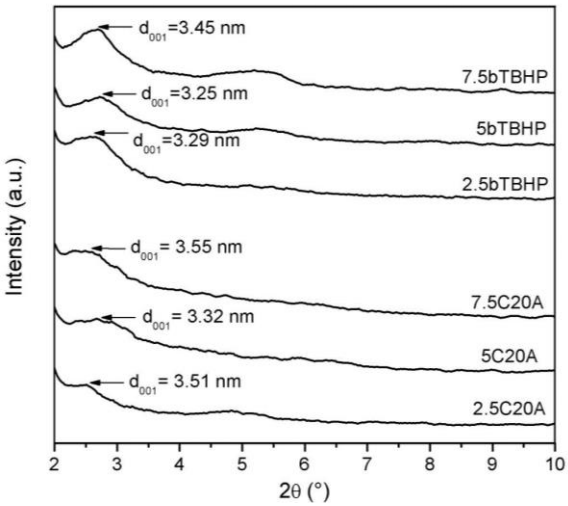

Fig. 1. XRD spectra of PCL based nanocomposites.

Several authors have found that the melt rheology of a polymeric matrix is strongly influenced by the incorporation of nanoparticles **[36-40]**. Thus, melt rheology can be useful to compare the clay dispersion degree of polymer/clay nanocomposites. This method has the advantages that the information obtained is representative of the whole sample instead of small zones of it and samples do not need to be specially conditioned **[41]**. Exfoliated or well-dispersed nanocomposites, including intercalated structures, increase the probability of edge to face and edge to edge interactions of the silicate platelets to occur, thus, it may build and mechanically stabilize mesoscale structures known as card-house **[31, 40]**. These structures promote a pseudo-solid like rheological behavior at low shear rates which results in pronounced shear thinning behavior in that zone of the melt rheological curves **[31, 40]**. It has been reported **[31, 42-44]** that the n_{Rh} parameter (see eq.3) increases as a function of the clay dispersion degree. Wagener *et al.* **[31]** have proposed n_{Rh} as a semi-quantitative measure of the clay dispersion degree of clay inside the sample. Semi-quantitative measure means that the average number of nanoplatelets per tactoid for a given nanocomposite cannot be calculated from n_{Rh} **[26]**. Even so, good correlation between n_{Rh} studied by melt rheology and clay dispersion degree analyzed by XRD and TEM for different polymer/clay nanocomposites was found by several authors **[26, 30-31]**. **Fig. 2** shows the melt rheology curves and resumes the values of the n_{Rh} parameter of the neat matrix and their nanocomposites. All nanocomposites showed a pronounced shear thinning behavior at shear rates in the range of 0.002-0.030 s^{-1}. On the other hand, the obtained n_{Rh} values are in accordance with those reported in a previous work for similar polymer/clay systems **[26]**. The tendencies found for the n_{Rh} values are in accordance with the XRD results, the C20A nanocomposites displayed higher n_{Rh} values than the bTBHP ones at the same clay content. This result confirms the improved clay dispersion degree of C20A inside the PCL matrix.

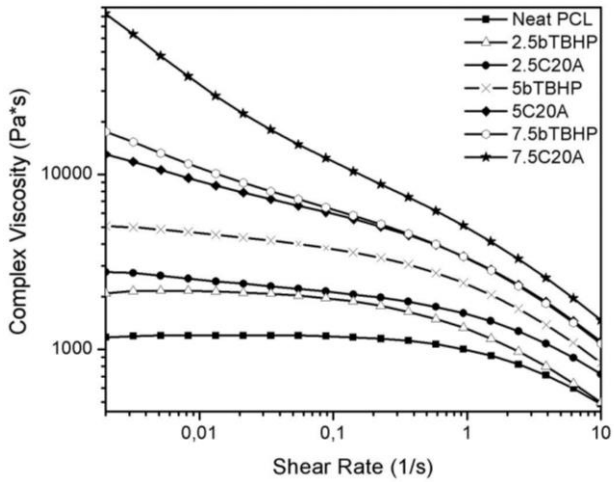

Fig. 2. Melt rheology curves of neat PCL and PCL/clay nanocomposites.

Fig. 3 (a-c) shows the SEM/TEM micrographs of the pure PCL and their 5 wt. % nanocomposites. In the case of 5C20A, no evidence of clay agglomeration is observed. Small bumps with an average diameter of 200 ± 20 nm, whose can be associated to clay agglomerates, were found in the 5bTBHP nanocomposite **(Fig. 3c)**. These results are in accordance with XRD and melt rheology characterization.

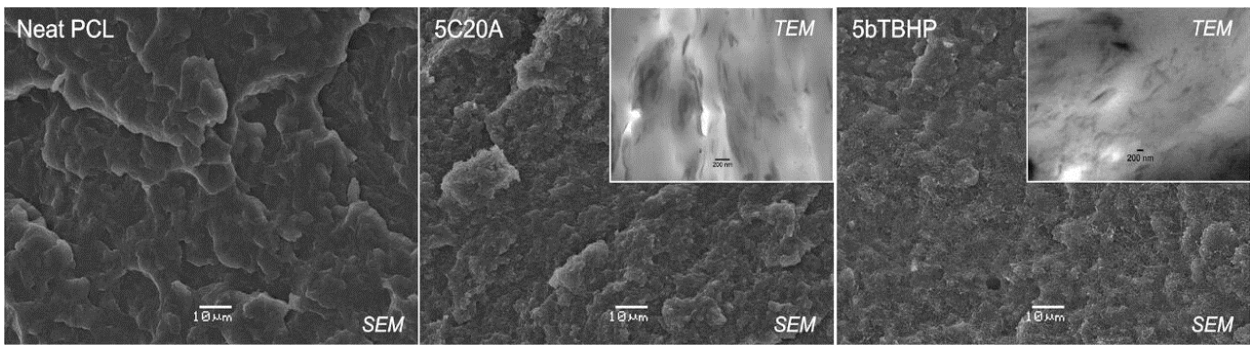

Fig.3. SEM and TEM micrographs of the pure matrix and PCL/organoclay nanocomposites.

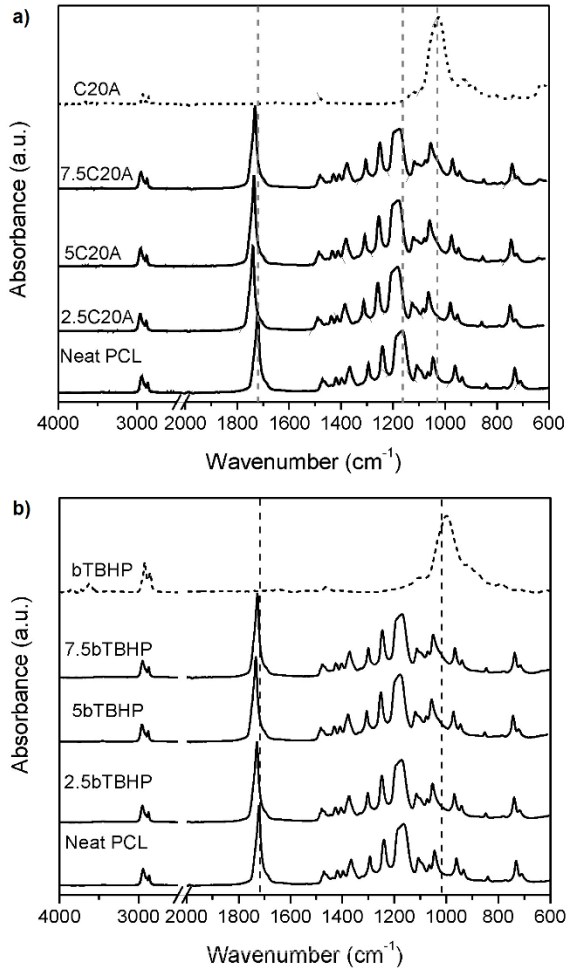

Fig. 4. FTIR spectra of PCL matrix and nanocomposites with different contents of organoclays: (a) C20A and (b) bTBHP.

Fig. 4 shows the FTIR spectra PCL/C20A (a) and PCL/bTBHP (b) nanocomposites compared with pure PCL and organoclay. Regarding pure PCL matrix, typical infrared peaks are observed **[45]**, including 2943 cm^{-1} (asymmetric CH_2 stretching), 2866 cm^{-1} (symmetric CH_2 stretching), 1721 cm^{-1} (carbonyl stretching), 1294 cm^{-1} (backbone C–O and C–C stretching in the crystalline phase), 1240 cm^{-1} (asymmetric COC stretching), 1190 cm^{-1} (OC–O stretching), and 1157 cm^{-1} (C–O and C–C stretching in the amorphous phase). Characteristic absorption bands of clay particles are observed at 3621 cm^{-1} (structural OH groups), 2926 and 2856 cm^{-1} (asymmetric and symmetric stretching vibrations C–H of CH_2 of the alkyl chain), 1658 cm^{-1} (OH stretching of free water adsorbed by the clay), 993 cm^{-1} (Si-O-Si in plane vibrations) **[46]**; 917 cm^{-1} (Al-O-H stretching vibration), 879 cm^{-1} (Mg-O-H vibration) **[47]**. Concerning PCL/bTBHP and PCL/C20A nanocomposites, the presence of clay is evidenced by a peak that appears at around 1026 cm^{-1}. It can be noted that this peak is more notorious for higher contents of both organo-clays. The interactions between PCL and the organoclay in the nanocomposites are evidenced in different zones of FTIR spectra: the C=O stretches, which appear at 1721 cm^{-1} for pristine PCL, shifted to 1737 cm^{-1}, 1734 cm^{-1} and 1728 cm^{-1} for 2.5, 5 and 7.5 wt.% C20A samples. Besides, the overlapped peaks at 1190 cm^{-1} and 1157 cm^{-1} also shift towards higher values, especially for the lowest content of C20A. These data imply the existence of hydrogen bonding interactions between PCL and the hydroxyl group in the organoclays. In general terms, the interactions are more evident for PCL/C20A samples than for PCL/bTHBP ones. This is also in accordance with the results obtained by XRD and rheology tests and the observations from SEM/TEM images.

Better clay dispersion degree for the C20A nanocomposites than bTBHP ones was not expected since the latter showed the strongest hydrophobicity, largest initial basal spacing and the strongest thermal stability, which are factors that should promote clay dispersion degree inside the PCL hydrophobic matrix mixed by melt blending. This behavior can be attributed to the highest organic content of the C20A clay. Therefore, it can be concluded that the balance between basal spacing, hydrophobicity, thermal stability and organic content of the neat clays, and the processing route will control the final clay dispersion degree of the nanocomposites.

In **Table 2**, it can be noticed that both organoclays did not significantly affect the Tm of pure PCL, whereas the crystallinity degree of PCL slightly increased when the organoclays were added. This observation suggests that the presence of the clay platelets may act as nucleating sites for the PCL crystallization **[8]**.

Table 2. Thermal and mechanical properties of PCL matrix and nanocomposites with different clay contents.

Clay content (wt.%)	PCL/C20A							PCL/bTBHP						
	Xcr (%)	*Tm* (ºC)	Residual mass (%)	$Td_{5\%}$ (°C)	E (MPa)	σ (MPa)	ε (%)	*Xcr* (%)	*Tm* (ºC)	Residual mass (%)	$Td_{5\%}$ (°C)	E (MPa)	σ (MPa)	ε (%)
0	61.5	62.1	0.1	324	193.4 ± 6.0	18.2 ± 0.9	1070 ± 278	61.5	62.1	0.1	324	193.4 ± 6.0	18.2 ± 0.9	1070 ± 278
2.5	63.4	60.0	1.9	308	231.1 ± 7.7	18.6 ± 0.4	790 ± 119	65.7	61.0	1.6	334	260.5 ± 9.7	18.5 ± 0.3	582 ± 283
5.0	64.3	61.5	3.6	310	169.3 ± 14.8	16.8 ± 0.2	850 ± 166	65.0	60.7	3.5	333	286.5 ± 24.4	17.9 ± 1.8	231 ± 78
7.5	64.7	60.1	5.3	317	191.7 ± 7.5	15.3 ± 1.8	427 ± 178	63.6	61.0	5.3	323	312.8 ± 32.3	17.0 ± 0.7	705 ± 174

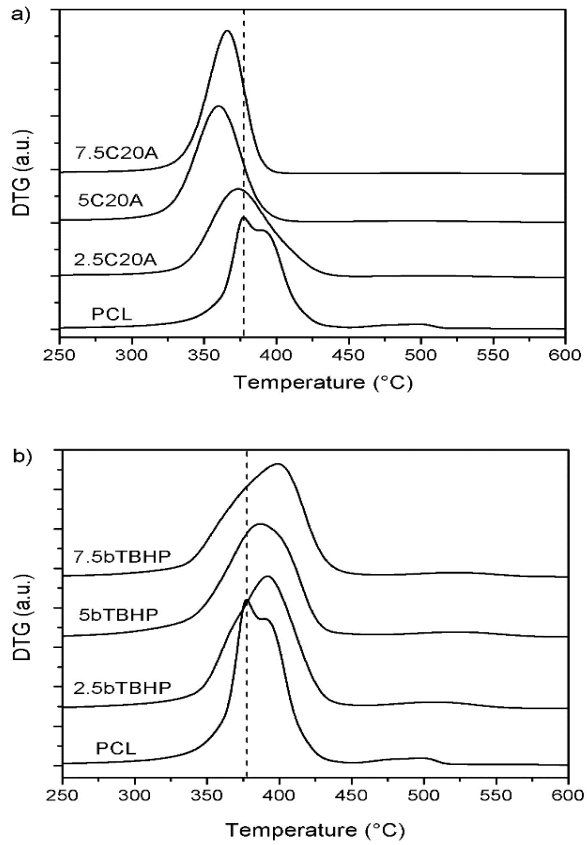

Fig. 5. DTGA curves of PCL matrix and nanocomposites with different contents of organoclay: (a) C20A; (b) bTBHP.

Regarding the thermal stability, it can be noticed in **Fig. 5** that PCL degrades in two stages. According to the literature, the first step, near 380 °C, corresponds to the random cleavage of the polyester chains via cis-elimination, followed by the unzipping depolymerization process near 400 °C **[48]**.

Moreover, from the observation of the $T_{d5\%}$ values in **Table 2** and the DTGA curves in **Fig. 5,** it can be deduced that the thermal degradation of PCL is affected by the presence of both organoclays. Regardless the type of organoclay, it can be noticed that all the nanocomposites degrade in only one step. Besides, the variations in the chemical composition of the organoclays was determinant for the degradation process observed in both composites. On the one hand, it is clear that the addition of quaternary alkylammonium modified clay within the PCL matrix, causes a reduction of the degradation temperature of the nanocomposites for all the clay loadings. This detrimental effect may be attributed to the fact that the layered silicates catalyze the PCL pyrolysis due to the presence of Lewis acidic sites formed by the degradation of the organic modifier **[49]**. On the other hand, in **Fig. 5 b** it can be noticed that the PCL/bTBHP nanocomposites exhibit slightly better thermal stability compared to pristine PCL. This can be attributed to the nature of the organic modifiers **[21]**, which is in accordance with the thermal stability of clay alone reported in Table 1 and with the dispersion of each clay inside PCL matrix previously described in Figs.1 to 3.

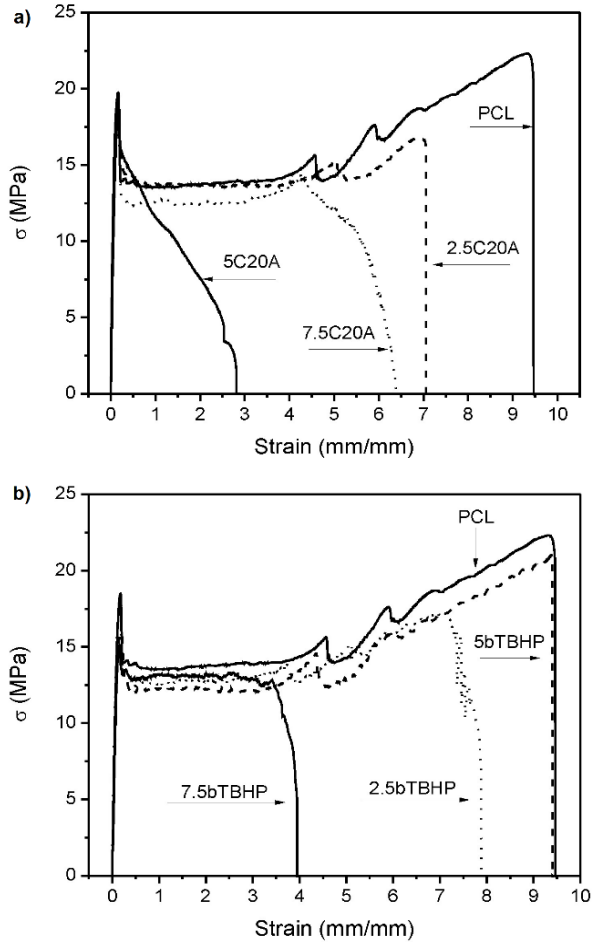

Fig. 6. Tensile stress-strain curves of PCL matrix and nanocomposites with different contents of organoclay: (a) C20A; (b) bTBHP.

Mechanical properties

The tensile stress–strain curves for the pristine PCL and the nanocomposites are shown in **Fig. 6** a (for the PCL/C20A nanocomposites) and b (for the PCL/bTBHP nanocomposites), and the values of Young´s modulus (E), tensile strength (σ) and strain at break (ε) are given in **Table 2**.

PCL/C20A nanocomposites showed higher Young´s modulus and tensile strength than PCL/bTBHP ones at the same clay content. The opposite trend was observed for the elongation at break. These results are a consequence of the improved clay dispersion degree obtained with the PCL/C20A nanocomposites; the correlation between clay dispersion degree and mechanical properties was widely demonstrated in the literature **[1, 9-10, 15, 26]**. The bTBHP organoclay showed the strongest hydrophobicity, the highest interlayer distance and the strongest processing stability, so better bTBHP dispersion inside the hydrophobic PCL matrix was expected but the opposite trend was observed; C20A showed better dispersion inside the PCL and hence improved mechanical properties. This result was attributed to the higher organic content of C20A.

Conclusion

In the present work, the effect of the type of clay modifier on the structure and properties of polycaprolactone (PCL)/organoclay nanocomposites was studied. Two organoclays were compared: a commercially available montmorillonite organoclay, C20A and a laboratory modified bentonite bTBHP. The bTBHP organo-clay showed the strongest hydrophobicity, the highest interlayer distance and the strongest thermal stability. Even so, PCL/bTBHP nanocomposites displayed poor clay dispersion degree and hence lower Young´s modulus and tensile strength than the PCL/C20A ones. The Young´s modulus of the PCL increased 62% after the incorporation of 7.5 wt.% of C20A, while the tensile strength and elongation at break did not change significantly. The results showed that the hydrophobicity, the interlayer distance and the processing stability of the clays are not enough to predict polymer/clay compatibility. In this case, the higher organic content of C20A can be controlling the final clay dispersion degree. Therefore, a balance between basal spacing, hydrophobicity, thermal stability and organic content of the neat clays, including the processing route, will control the final clay dispersion degree of the nanocomposites.

Acknowledgements

Authors acknowledge to National Scientific and Technical Research Council (CONICET) (PIP 00617), National Agency for the Promotion of Science and Technology (ANPCyT) (FS Nano 004), and the National University of Mar del Plata (UNMdP) (ING392/14) for the financial support.

Author's contributions

Authors have no competing financial interests.

References

1. Lepoittevin B.; Devalckenaere, M.; Pantoustier, N., Alexandre, M.; Kubies, D.; Calberg, C.; Jérôme, R.; Dubois, P.; *Polymer*, **2002**, 43, 4017. **DOI:** 10.1016/S0032-3861(02)00229-X
2. Chen, B.; Evans, J. R. G.; *Macromolecules*, **2006**, 39, 747. **DOI:** 10.1021/ma052154a: 10.1021/ma052154a
3. Kojima, Y.; Usuki, A.; Kawasumi, M.; Okada, A.; Fukushima, Y.; Kurauchi, T.; Kamigaito, O.; *J. Mater. Res.*, **1993**, 8, 1185. **DOI:** 10.1557/JMR.1993.1185
4. Sinha Ray, S., Bousmina, M.; *Prog. Mater. Sci.*, **2005**, 50, 962. **DOI:** 10.1016/j.pmatsci.2005.05.002
5. Kunioka, M.; Ninomiya, F.; Funabashi, M.; *Polym. Degrad. Stab.*, **2007**, 92, 1279. **DOI:** 10.1016/j.polymdegradstab.2007.03.028
6. Singh, N. K.; Purkayastha, B. D.; Roy, J. K.; Banik, R. M.; Yashpal, M.; Singh, G.; Malik, S.; Maiti, P.; *ACS Appl. Mater. Interfaces*, **2009**, 2, 69. **DOI:** 10.1021/am900584r
7. Homminga, D.; Goderis, B.; Dolbnya, I.; Groeninckx G. *Polymer*, **2006**, 47, 1620. **DOI:** 10.1016/j.polymer.2005.12.080
8. Yahiaoui, F.; Benhacine, F.; Ferfera-Harrar, H.; Habi, A.; Hadj-Hamou, A.; Grohens. Y.; *Polym. Bull.*, **2015**, 72, 235. **DOI:** 10.1007/s00289-014-1269-0
9. Ludueña, L. N.; Alvarez, V. A.; Vazquez. A.; *Mater. Sci. Eng, A*, **2007**, 460-461, 121. **DOI:** 10.1016/j.msea.2007.01.104
10. Messersmith, P. B.; Giannelis E. P.; *J Polym Sci, Part A: Polym. Chem.*, **1995**, 33, 1047. **DOI:** 10.1002/pola.1995.080330707
11. Gilman, J. W.; Jackson, C. L.; Morgan, A. B.; Harris, R.; Manias, E.; Giannelis, E. P.; Wuthenow, M.; Hilton, D.; Phillips, S. H.; *Chem. Mater.*, **2000**, 12, 1866. **DOI:** 10.1021/cm0001760: 10.1021/cm0001760
12. Gorrasi, G.; Tortora, M.; Vittoria, V.; Pollet, E.; Lepoittevin, B.; Alexandre, M.; Dubois. P.; *Polymer*, **2003**, 44, 2271. **DOI:** 10.1016/s0032-3861(03)00108-3
13. Zhang, Z.; Yang, J.-L.; Friedrich, K.; *Polymer*, **2004**, 45, 3481. **DOI:** 10.1016/j.polymer.2004.03.004
14. Roelofs, J. C. A. A.; Berben P. H.; *Appl. Clay Sci.*, **2006**, 33, 13. **DOI:** 10.1016/j.clay.2006.03.001
15. Alexandre, M.; Dubois. P.; *Mater. Sci. Eng. R Rep.*, **2000**, 28, 1. **DOI:** 10.1016/s0927-796x(00)00012-7
16. Pantoustier, N.; Lepoittevin, B.; Alexandre, M.; Dubois, P.; Kubies, D.; Calberg, C.; Jérôme R.; *Polym. Eng. Sci.*, **2002**, 42, 1928. **DOI:** 10.1002/pen.11085: 10.1002/pen.11085
17. Fischer, H.; *Mater. Sci. Eng., C*, **2003**, 23, 763. **DOI:** 10.1016/j.msec.2003.09.148
18. Bergaya, F.; Detellier, C.; Lambert, J. F.; Lagaly, G., in *Developments in Clay Science*; (Ed: Faïza, B.; Gerhard, L.), Elsevier, **2013**, 5, pp. 655. **DOI:** 10.1016/B978-0-08-098258-8.00020-1
19. Picard, E.; Gauthier, H.; Gérard, J. F.; Espuche, E.; *J. Colloid Interface Sci.*, **2007**, 307, 364. **DOI:** 10.1016/j.jcis.2006.12.006
20. Xi, Y.; Frost, R. L.; He, H.; *J. Colloid Interface Sci.*, **2007**, 305, 150. **DOI:** 10.1016/j.jcis.2006.09.033
21. Xie, W.; Xie, R.; Pan, W. P.; Hunter, D.; Koene, B.; Tan, L. S. R.; Vaia. *Chem. Mater.*, **2002**, 14, 4837. **DOI:** 10.1021/cm020705v
22. Bergaya, F.; Jaber, M.; Lambert, J.-F., in *Rubber-Clay Nanocomposites*; (Ed: Galimberti, M.), John Wiley & Sons, Inc., **2011**, pp. 45. **DOI:** 10.1002/9781118092866.ch1
23. Drown, E. K.; Mohanty, A. K.; Parulekar, Y., Hasija, D.; Harte, B. R.; Misra, M.; Kurian, J. V.; *Compos. Sci. Technol.*, **2007**, 67, 3168. **DOI:** 10.1016/j.compscitech.2007.04.011
24. Janigová, I.; Lednický, F.; Mošková, D. J.; Chodák, I.; *Macromol. Symp.*, **2011**, 301, 1. **DOI:** 10.1002/masy.201150301
25. Zheng, X.; Wilkie, C. A.; *Polym. Degrad. Stab.*, **2003**, 82, 441. **DOI:** 10.1016/s0141-3910(03)00197-6
26. Ludueña, L. N.; Kenny, J. M.; Vázquez, A.; Alvarez, V. A.; *Mater. Sci. Eng., A* **2011**, 529, 215. **DOI:** 10.1016/j.msea.2011.09.020
27. Ludueña, L. N.; Vázquez, A.; Alvarez, V. A., *J. Appl. Polym. Sci.*- **2013**, 128, 2648. **DOI:** 10.1016/j.msea.2011.09.020
28. Ollier, R.; Vazquez, A.; Alvarez V.; in *Advances in Nanotechnology*; (Eds: Bartul, Z.; Trenor, J.), Nova Science Publishers; USA, **2011**, 10, pp. 281.
29. D'Amico, D. A.; Ollier, R. P.; Alvarez, V. A., Schroeder, W. F.; Cyras, V. P.; *Appl. Clay Sci.*, **2014**, 99, 254. **DOI:** 10.1016/j.clay.2014.07.002
30. Yam, W.; Ismail, J.; Kammer, H.; Schmidt, H.; Kummerlöwe, C.; *Polymer*, **1999**, 40, 5545. **DOI:** 10.1016/S0032-3861(98)00807-6
31. Wagener, R.; Reisinger, T. J. G.; *Polymer*, **2003**, 44, 7513. **DOI:** 10.1016/j.polymer.2003.01.001
32. Ollier, R.; Lanfranconi, M.; Alvarez V.; in *Advances in Materials Science Research.*; (Ed: Wythers, M. C.), Nova Science Publishers: USA, **2014**, 17, pp. 55.
33. Abdallah, W.; Yilmazer. U; *J. Appl. Polym. Sci.*, **2013**, 128, 4283. **DOI:** 10.1002/app.38651
34. Suin, S.; Khatua B. B.; *Ind. Eng. Chem. Res.*, **2012**, 51, 15096. **DOI:** 10.1021/ie302209x
35. Mittal; V.*J; Thermoplast. Compos. Mater,*. **2013**, 26, 1082. **DOI:** 10.1177/0892705711433439

36. Manitiu, M.; Horsch, S.; Gulari; E., Kannan, R. M.; *Polymer*, **2009**, 50, 3786.
DOI: 10.1016/j.polymer.2009.05.036
37. Franchini, E.; Galy, J.; Gérard, J.-F.; *J. Colloid Interface Sci.*, **2009**, 329, 38.
DOI: 10.1016/j.jcis.2008.09.020
38. Krishnamoorti, R.; Vaia, R. A.; Giannelis, E. P.; *Chem. Mater.*, **1996**, 8, 1728.
DOI: 10.1021/cm960127g
39. Krishnamoorti, R., Giannelis, E. P.; *Macromolecules* **1997**, 30, 4097.
DOI: 10.1021/ma960550a
40. Ren, J.; Silva, A. S.; Krishnamoorti, R.; *Macromolecules* **2000**, 33, 3739.
DOI: 10.1021/ma992091u
41. Ahmed, J.; Auras, R.; Kijchavengkul, T.; Varshney, S. K.; *J Food Eng.*, **2012**, 111, 580.
DOI: 10.1016/j.jfoodeng.2012.03.014
42. Zhao, J.; Morgan, A. B.; Harris, J. D.; *Polymer*, **2005**, 46, 8641.
DOI: 10.1016/j.polymer.2005.04.038
43. Krishnamoorti, R.; Ren, J.; Silva, A. S.; *J. Chem. Phys.*, **2001**, 114, 4968.
DOI: 10.1063/1.1345908
44. Durmus, A.; Kasgoz, A.; Macosko, C. W.; *Polymer*, **2007**, 48, 4492.
DOI: 10.1016/j.polymer.2007.05.074
45. Elzein, T., Nasser-Eddine, M.; Delaite, C.; Bistac, S.; Dumas, P.; *J. Colloid Interface Sci.*, **2004**, 273, 381.
DOI: 10.1016/j.jcis.2004.02.001
46. Farmer, V. C.; in *The Infra Red Spectra of Clay Minerals*; (Ed: Farmer, V. C.), Mineralogical Society, London, **1974**, 4, pp. 331.
47. Madejová, J.; *Vib. Spectrosc.*, **2003**, 31, 1.
DOI: 10.1016/S0924-2031(02)00065-6
48. Persenaire, O.; Alexandre, M.; Degée, P.; Dubois, P.; *Biomacromolecules*, **2001**, 2, 288.
DOI: 10.1021/bm0056310
49. Bellucci, F.; Camino, G.; Frache, A.; Sarra, A.; *Polym. Degrad. Stab.*, **2007**, 92, 425.
DOI: 10.1016/j.polymdegradstab.2006.11.006

